Journal of Hydraulic Structures
J. Hydraul. Struct., 2024;10(3):1-17
DOI: 10.22055/jhs.2024.44697.1261

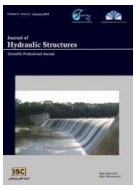

OPEN ACCESS

Investigating the effect of buried walls through rockfill detention structures on the longitudinal water surface profile

Jafar Chabokpour [*1]
Omar Minaei [1]

Abstract

Rockfill structures in river training projects, such as detention dams, gabions, and levees, play a significant role in flood control. One of the common types of these structures is porous flood mitigation dams. This research investigated the surface flow profile by developing an analytical model based on specific energy relationships and Wilkins pore velocity and employing numerical methods based on estimation and correction methods. In order to examine the efficiency of the presented models, experiments were performed both with and without buried inside walls through rockfill media. The results show the accuracy and efficiency of analytical and numerical methods for calculating the water surface profile. The numerical estimation-correction method is used to estimate the passing flow profile through the rockfill media. In order to apply these methods in the experiments including buried curtain, the profile is divided into two parts, and the computations were done by considering two boundary conditions at the outlet and the buried wall position. The flow profile was calculated by the least square curve fitting method, and the c and d coefficients were extracted by taking into account the influencing factors, including the rockfill media diameter, the length of the porous medium, and operated flow rate for a specific diameter. Moreover, the results indicate the appropriate correlation between the laboratory data and analytical and numerical solutions in the experiments, including wall. Quantitatively, the root mean square error (RMSE) ranged from 3 to 5.5 mm, with a relative error between 3 and 9.3%. The relative error increased with higher core heights, particularly downstream of the core due to local flow acceleration and significant flow curvature. At a flow discharge of 0.19 l/s, the relative error was 3%, rising to 8% at higher flow rates. It was also observed that with the increase of the entrance flow discharge, the profile estimation accuracy decreased, and curvature in the water surface profile was observed.

Keywords: Rockfill Dam, Water Surface Profile, Analytical Solution, Numerical Estimation-Correction Method, Vertical and Inclined Curtains.

Received: 02 September 2023; Accepted: 09 April 2024

[*] E-mail: J.chabokpour@maragheh.ac.ir (**Corresponding Author**)
[1] Department of Civil Engineering, University of Maragheh, Maragheh, Iran.

1. Introduction

In large porous media, flow can occur in different ways depending on the characteristics of the medium. In some cases, when the fluid velocity increases or the pore size decreases, the flow behavior can deviate from Darcy flow. This is known as non-Darcy flow and is characterized by inertial, viscous, or turbulent effects, which can result in a non-linear relationship between flow rate and pressure gradient. Understanding and predicting the flow through large porous media is crucial in many fields, including hydrology, geology, environmental science, and petroleum engineering. It helps in determining the movement of contaminants in groundwater, designing efficient drainage systems, optimizing oil and gas recovery, and modeling the transport of pollutants in the subsurface. Rock embankments are used as a crucial part of gravel structures. Unlike the concrete and earth dams built through river reaches, gravel structures have much lower costs compared to them. One of the most important advantages of these structures is their use as flood mitigation structures. These detention structures are usually built in series. By forming small reservoirs through the river, they cause flood storage through the river reaches. The passing flood through large porous media has a high pore velocity and is therefore known as None-Darcy flow. By increasing the flow velocity inside the pore system, the inertial force gradually overcomes the viscous force, and consequently, the turbulent None-Darcy flow occurs [1-3]. Non-Darcy flows can be classified into two categories: parallel flows and radial flows. Parallel flows are commonly observed in scenarios involving gravel dams, gabions, and other similar structures. In these cases, the streamlines are nearly parallel, and the flow can exist in both pressurized and free-surface modes. On the other hand, radial flows are encountered in situations such as wells drilled in coarse-grained alluvial beds. These flows require specialized analysis techniques to understand their behavior and impact on hydraulic structures [4-6].

Buried streams, which are often formed due to mining or roadway operations near rivers, present unique challenges in hydraulic engineering. These streams can alter the flow regime from open channel flow to non-Darcy inner flow, making it essential to accurately predict and simulate the flow patterns. Gradually-varied flow algorithms offer a practical and cost-effective approach to studying the flow in buried streams, providing valuable insights for design and operational considerations [7-9]. The gradually-varied flow theory is a widely used approach in analyzing and simulating flow in non-Darcy porous media. This theory requires less data compared to solving complex equations such as the Parkin equation, making it more practical and cost-effective. By applying the gradually-varied flow theory, researchers have successfully calculated water surface profiles in various scenarios, including radial non-Darcy flow with a free surface [10-13].

In addition to experimental approaches, numerical methods have also been employed to estimate water surface profiles in buried streams. Researchers have utilized techniques such as finite differences, finite elements, and finite volumes to solve the equations governing radial non-Darcy flow. These numerical methods require extensive data and computational resources, but they provide valuable insights into the behavior of flow in porous media [14].

One-dimensional analysis using the gradually-varied flow theory and two-dimensional analysis using the Parkin equation have been extensively used in studying non-Darcy flows. However, the gradually-varied flow theory offers advantages in terms of data requirements and computational complexity. The water surface profile obtained from the gradually-varied flow theory can serve as a crucial boundary condition for solving the Parkin equation, simplifying the overall analysis process [15, 16].

The equations that relate the velocity and hydraulic gradient to each other are in two general forms: quadratic and power. In order to more successfully model the turbulence in the pore system, Forchheimer added a quadratic term to Darcy's Equation to model both turbulent and viscous flow efficiently. In other words, if any of these two mechanisms are powerful, the corresponding coefficients would be more prominent. The equation's general form is according to Eq. 1 [10].

$$i = a.V + b.V^2 \quad (1)$$

In which $i$is hydraulic gradient, $V$is flow velocity and a, $b$are equation parameters.

Eq. 1 has two coefficients, and Eqs. 2 and 3 are presented for its parameters using dimensional analysis for one-dimensional [17, 18].

$$a = \frac{\mu}{\rho g k} \quad (2)$$

$$b = \frac{1}{g\sqrt{ck}} \quad (3)$$

As a result, if Forchheimer's Equation is rewritten using mentioned coefficients, the following relation can be obtained.

$$i = \frac{\mu}{\rho g k}V + \frac{1}{g\sqrt{ck}}V^2 = \frac{\mu}{\rho g}[\frac{1}{k} + \frac{\rho}{\mu\sqrt{ck}}V]V \quad (4)$$

In which μ is the dynamic viscosity, g is the acceleration of gravity, k is the intrinsic permeability, V is the apparent velocity, ρ is the fluid density, and c is the experimental constant coefficient.

In previous studies, it is typical to use the actual pore velocity instead of the average velocity. Therefore, by using it and defining the j function as Eq. 5, Eq. 6 can be extracted.

$$j = \frac{1}{\frac{1}{k} + \frac{\rho V_a}{\mu\sqrt{c'k'}}} \quad (5)$$

$$i = i_t = \frac{\mu}{\rho g j}V_a \quad (6)$$

In Eqs.5 and 6, c' and k' are similar parameters to c and k, and they can be obtained better by applying the actual velocity (V_a) instead of the average velocity (V). However, in the Darcy flow, the equality $j = k$ is valid [19-21].

The next group of equations that relate the hydraulic gradient to the pore flow velocity are power-form equations, and one of the most widely used equations is presented by Wilkins (1956) [20] as Eq. 7.

$$V_V = C\mu^a m^b i^\omega \quad (7)$$

Where: V_V is passing pore velocity, C is an experimental constant that can be determined according to the shape of the particles, μ is the dynamic viscosity of water, and a, b are coefficients that are determined experimentally and using laboratory data.

Wilkins calibrated and validated the general form of Eq. 7 by conducting experiments on coarse-grained materials, and consequently, Eq. 8 is obtained.

$$V_v = Wm^{0.5} i^{0.54}, \qquad i = Cv_v^d \tag{8}$$

$Wm^{0.5}$ is assumed as the hydraulic conductivity of the porous media and the value of 0.54 was estimated as the power of the hydraulic gradient because of turbulent flow conditions [22].

Heydari et al., [23] discussed the longitudinal profile of the non-Darcy flow using the finite element numerical method and presented an equation for the flow rate. Using experimental data and their analysis, Sedeghi Asal et al., [22] indicated that in horizontal and gentle slopes, the passing flow through large porous media follows the gradually varied flow theory. In contrast, in the steep slopes, The gravity force in the flow direction is higher; consequently, uniform flow forms. Salahi et al., [24] based on a laboratory study on different types of crushed and angular rock materials in a wide range of Reynolds numbers, presented values for the power of the Wilkins equation. The results of their research showed that the velocity power in the Wilkins relation fluctuates in the range of 1.6 to 1.8 depending on the grain size characteristics. Asiban et al., [25] calculated the longitudinal profile of the flow using the direct step-by-step method, mostly used in subcritical flows. As a result, the relative error percentage for profile estimation was calculated as 17.6%.

Sarvarian et al., [26] in their study optimized the location and arrangement of rockfill dams in Taleghan basin using both economic and hydraulic criteria. The study employed the "BRM" model (Basin Routing Model, a program developed in Matlab to calculate flow through rockfill dams and estimate the outlet hydrograph of a basin) and the NSGAII method (Non-dominated Sorting Genetic Algorithm II, a multi-objective optimization algorithm used in the study) for optimization. Results showed a 74.4% cost reduction and a 64.9% peak discharge reduction compared to alternative scenarios. Most dams were placed upstream and on the main river to enhance flood control efficiency [26].

Zhang et al., [27] discussed the analytical treatment of non-Darcian flow near a non-uniform flux well face, highlighting limitations in the linearization method for turbulent flow. Their study emphasized no direct analysis of datasets.

Chabakpour and Amiri [3] investigated the application of the GVF flow equation for profile estimation of passing flow through the porous media using direct numerical methods. For this purpose, numerical methods of Euler, modified Euler, and 4th-order Range-Kutta were used, and the results were compared with the experimental data. It was concluded that the Euler method has low accuracy and is unsuitable for flow profile calculation. Also, the 4th-order Range-Kutta method is more accurate than the modified Euler method. Furthermore, the c and d coefficients were considered equal to 22.5 and 2, respectively, indicating a completely turbulent flow.

Considering previous studies, it can be seen that the hydraulic investigations of passing flows through large porous media have been of interest to many previous researchers, and the operated numerical methods have had favorable results. However, due to the nature of gravel dams (for flood mitigation), they differ somewhat from the investigated cases. In order to increase their applicability, concrete or clay, buried curtains are placed inside their body. These walls, whether vertical or inclined, affect the profile of the upstream return flow and practically divide the longitudinal profile into two different parts. For this reason, this research attempted to

investigate the issue in more detail by building a laboratory model, extracting analytical relationships, and using numerical methods. The analysis can also include comparing the performance of detention structures with and without buried walls in term of water surface profiles. Additionally, physical or laboratory experiments can be conducted to investigate the effect of buried walls on the water surface profile. These experiments can involve constructing scaled-down models of the detention structure, including the buried walls, and measuring the resulting water surface profiles under controlled flow conditions. Overall, investigating the effect of buried walls through rockfill detention structures on the longitudinal water surface profile requires a combination of hydraulic modeling, empirical analysis, and physical experiments.

2. Materials and methods

2.1. Laboratory apparatus

The current study used a laboratory flume with a length of 180 cm, width of 20 cm, and height of 70 cm (Fig.1). The flume has a horizontal bed, and different hydraulic gradients were created by flow variation at the porous media entrance. For this purpose, the flow profiles inside the porous medium were determined by operating three entrance discharges of 0.19, 0.26, and 0.37 (l/s). Glass sheets with heights of 10, 20, 30, 40, and 50 cm were used to create an impermeable core. The sheets with a height of 10, 20, and 30 cm were operated as vertical cores at distances of 45, 68, and 90 cm (from the media entrance). On the other hand, the sheets with heights of 40 and 50 cm were operated as inclined cores with slopes of 1:3, 1:2, and 1:1. It should be noted that each of the mentioned cores with heights of 10, 20, and 30 cm (shown with the letters S1, S2, and S3) can be positioned at places of 1, 2, and 3 (which are displayed with the letters P1, P2, and P3). Also, S4 and S5 cores were installed in P4 and P5 positions (Fig. 1). Rockfill materials with an average diameter of 1.8 cm and a uniformity coefficient of 1.4 were used to operate the experiments. In Table 1, the different characteristics of experiments are presented at a flow discharge of 0.26 l/s.

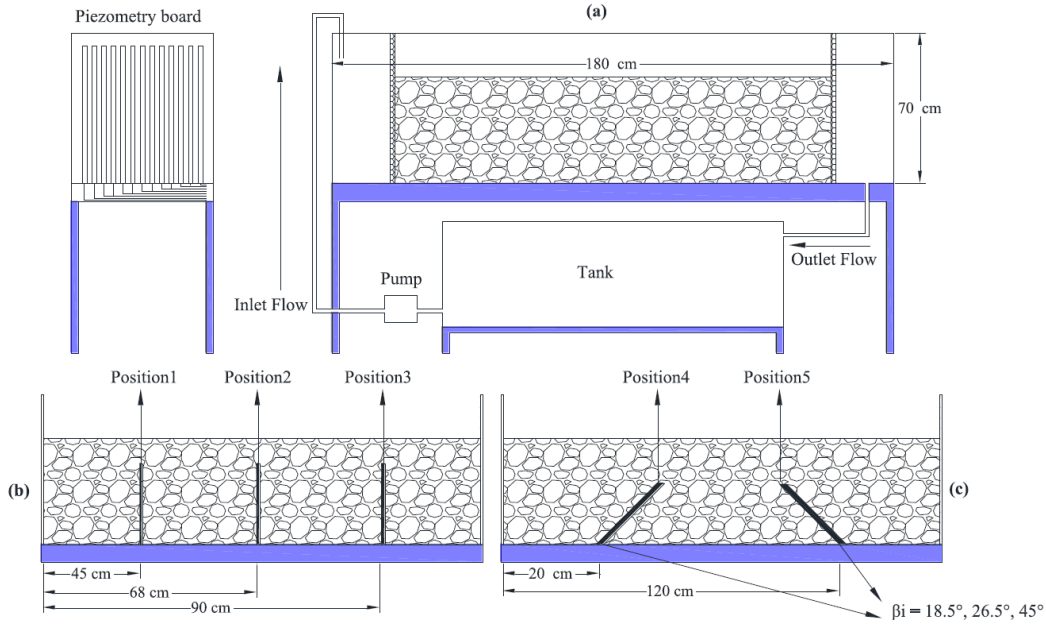

Figure 1. General schematic of the laboratory flume and the placement of glass plates through rockfill media, a) Laboratory flume, b) Position of S1, S2, and S3 as vertical cores, c) Position of S4 and S5 as inclined cores

Table. 1. General characteristics of the conducted experiments at a flow rate of 0.26 l/s

Downstream flow depth (cm)	Upstream flow depth (cm)	Core angle (degree)	Core position	Core height (cm)	Core	Experiment NO.
1	11.9	90	P1	10	S1	1
1.1	12.4	90	P2	10	S1	2
1.4	13.1	90	P3	10	S1	3
1.5	21.7	90	P1	20	S2	4
2.2	22.1	90	P2	20	S2	5
1.1	22	90	P3	20	S2	6
1.8	31.6	90	P1	30	S3	7
1.1	31.4	90	P2	30	S3	8
1.1	31.5	90	P3	30	S3	9
1.8	17.8	18.5	P4	40	S4	10
2	21.4	26.5	P4	40	S4	11
2.2	31.8	45	P4	40	S4	12
3	16.9	18.5	P5	40	S4	13
3.2	21.5	26.5	P5	40	S4	14
2.8	30.9	45	P5	40	S4	15
2.1	20.5	18.5	P4	50	S5	16
2	25.5	26.5	P4	50	S5	17
2.6	38.4	45	P4	50	S5	18
3.2	19.3	18.5	P5	50	S5	19
3	24.6	26.5	P5	50	S5	20
2.8	34.6	45	P5	50	S5	21

2.2. Analytical solution extraction

In large porous media, the flow behavior can vary depending on factors such as the size and connectivity of the pores, the fluid viscosity, and the presence of any obstructions or impurities within the media. Generally, the flow tends to be slower in larger pores with higher permeability, while smaller pores or obstructions can hinder the flow or lead to channeling effects. The gradually varied flow equation in rockfill media is an equation that is used to calculate the variation of water depth and velocity in open channel flow through a rockfill material. It takes into account the hydraulic resistance and roughness characteristics of the rockfill material. This equation is based on the principles of conservation of mass and momentum in open channel flow and is used to analyze and design rockfill channels, such as those found in dams or spillways. It allows engineers to determine the water depth and velocity under different flow conditions, which is important for ensuring proper functioning and stability of the rockfill media. It is possible to use fractional and power equations, especially the Wilkins pore velocity relation. Using power form equations simplifies the integration and is more acceptable in practice. Assuming uniform flow formation, the specific energy equation can be written as Eq. 9 [28].

$$E = y + \frac{V^2}{2g} = y + \frac{q^2}{2gn^2y^2} \tag{9}$$

Where E is the specific energy, y is the flow depth, n is the porous media porosity, and q is the flow rate per unit width. By differentiating both sides of Eq. 9, Eq. 10 can be obtained.

$$\frac{dE}{dx} = \frac{dy}{dx}\left(1 - \frac{q^2}{gn^2y^3}\right) \quad (10)$$

The power form of hydraulic velocity and gradient in non-Darcy flows is also according to Eq. 11, and Eq. 12 is obtained by taking the derivative of specific energy with respect to longitudinal distance.

$$i = a(\frac{q}{ny})^b \quad (11)$$

$$\frac{dE}{dx} = i = a(\frac{q}{ny})^b \quad (12)$$

Also, Eq. 13 can be achieved by integrating Eq. 12.

$$\int_{y1}^{y}\left(y^b - \frac{q^2}{gn^2y^{3-b}}\right)dy = \int_{x1}^{x} a(\frac{q}{n})^b dx \quad (13)$$

Finally, the result of integration can be shown as Eqs. 14 and 15.

$$\frac{y^{1+b}-y_1^{1+b}}{1+b} - \frac{q^2}{gn^2(b-2)}(y^{b-2} - y_1^{b-2}) = a\left(\frac{q}{n}\right)^b (x - x_1) \quad (14)$$

$$\frac{y^{1+b}}{1+b} + \frac{q^2}{gn^2(b-2)}(y^{b-2}) = a\left(\frac{q}{n}\right)^b (x - x_1) + \frac{q^2}{gn^2(b-2)}y_1^{b-2} + \frac{y_1^{1+b}}{1+b} \quad (15)$$

If the values of a, b, n, and q are known, the water surface profile can be calculated using Eq. 15 by applying exit flow depth from the porous media as downstream boundary conditions. Eq. 15 can be operated as the method of calculating distance in terms of depth or depth in terms of distance. For turbulent flow, which is typical to large porous media, by assuming b coefficient equal to 2 in the Wilkins equation, Eq. 15 is rewritten to the simplified form of Eq. 16.

$$\mathrm{y} = \left(y_1^3 + 3a\left(\frac{q}{n}\right)^2 (x - x_1)\right)^{\frac{1}{3}} \quad (16)$$

2.3. Operated Numerical Solution

The gradually varied flow is dominant for passing through large porous media Eq. 17.

$$\frac{dy}{dx} = f(x,y) = \frac{S_0 - S_f}{1 - (\frac{\alpha BQ^2}{gA^3})} = \frac{S_0 - S_f}{1 - Fr^2} \quad (17)$$

Where $\frac{dy}{dx}$ shows the depth variation rate in the flow direction, S_0 is the longitudinal slope, S_f energy line slope, α is the velocity correction factor, Q is the flow discharge, B is the flow width, A is the cross-sectional flow area, and g is the gravity acceleration.

In Eq. 17, due to the horizontality of the channel bed, the value of $S_0$is equal to zero, and the value of $S_f$is equal to the value of the hydraulic gradient (i). Also, the i value was extracted using Eq. 8. Advanced numerical methods are classified into two categories: single-step methods and estimation-correction methods.

The current study used the estimation-correction method to estimate the passing flow profile through the rockfill media. In the estimation-correction methods, an uncertain depth is first estimated using one-step methods and then corrected to reach the desired accuracy. Then, based on the resulting corrected depth, the next depth is estimated and then corrected [29]. In the estimation part, one-step methods can be used. In the present study, Euler's method was used for this stage as Eqs. 18.

$$y_{i+1}^{(0)} = y_i + f(x_i, y_i)\Delta x \tag{18}$$

$$f(x_i, y_i) = \frac{-S_{fi}}{1 - (\frac{B_i \times Q^2}{g \times A_i^3})} = \frac{-S_{fi}}{1 - Fr_i^2} \tag{19}$$

$$\Delta x = x_{i+1} - x_i \tag{20}$$

Using Eq. 18, the first flow depth is estimated. Other parameters of Eq. 18 are also estimated from Eq. 19 and Eq.20. The zero power on the left side of the equation represents the first estimate. Yi is the boundary condition, and laboratory data obtain its value. Considering that the boundary condition of subcritical flows is downstream, yi in the first estimate was considered the exit depth from rockfill media. The first estimate is corrected in the next step according to Eq. 21.

$$\boldsymbol{y_{i+1}^{(1)} = y_i + \frac{1}{2}\left[f(x_i, y_i) + f\left(x_{i+1}, y_{i+1}^{(0)}\right)\right]\Delta x} \tag{21}$$

The depth modification continues such that the jth modification is according to Eq. 22.

$$\boldsymbol{y_{i+1}^{(j)} = y_i + \frac{1}{2}\left[f(x_i, y_i) + f\left(x_{i+1}, y_{i+1}^{(j-1)}\right)\right]\Delta x} \tag{22}$$

The depth correction continues until the calculated depth difference in correction j and j-1 is negligible. The flow depth at point xi+2 is calculated and corrected in the next step according to the above-mentioned method.

2.4. Statistical criteria for validity checking of the employed methods

To compare the experimental and numerical results, statistical methods of root mean square error (RMSE), mean absolute error (MAE), relative error (RE), and coefficient of determination (R^2) were operated according to Eqs. (23-26).

$$RMSE = \sqrt{\frac{\sum_{i=1}^{n}(X - Y)^2}{n}} \tag{23}$$

$$MAE = \frac{1}{n}\sum_{i=1}^{n}|X - Y| \tag{24}$$

$$MAPE = \frac{100}{n}\sum_{i=1}^{n}\left|\frac{X - Y}{X}\right| \tag{25}$$

$$R^2 = \left[\frac{\sum_{i=1}^{n}(X_i - \overline{X}) \cdot (Y_i - \overline{Y})}{\sqrt{\sum_{i=1}^{n}(X_i - \overline{X})^2 \cdot \sum_{i=1}^{n}(Y_i - \overline{Y})^2}} \right]^2 \quad (26)$$

In the above Eqs, n is the data number, X is the laboratory data, Y is the calculated data, $\bar{X}$ is the average of the observed data, and $\bar{Y}$ is the average of the calculated data.

3. Results and discussion

3.1. Flow profile in non-core states

In order to check the flow profiles by the estimation-correction method and estimate the appropriate value for c and d coefficients in Eq.8, first, the flow passing inside porous media without core was investigated. According to the provided range by previous researchers and using the trial and error method, the values of c and d coefficients were considered equal to 22.5 and 1.62, respectively. The experimental and numerical data comparison is shown in Fig. 2 at flow rates of 0.26 and 0.37 l/s, and the error criteria can be seen in each figure.

As shown in Fig. 2, the error values are acceptable, and the calculated results are close to the laboratory data. The RMSE value was calculated between 0.5 and 0.7 cm. Also, the average value of the relative error for all four tests was calculated to be approximately 7.5%. Fig. 3 shows measured depths versus calculated depths by the estimation-correction method.

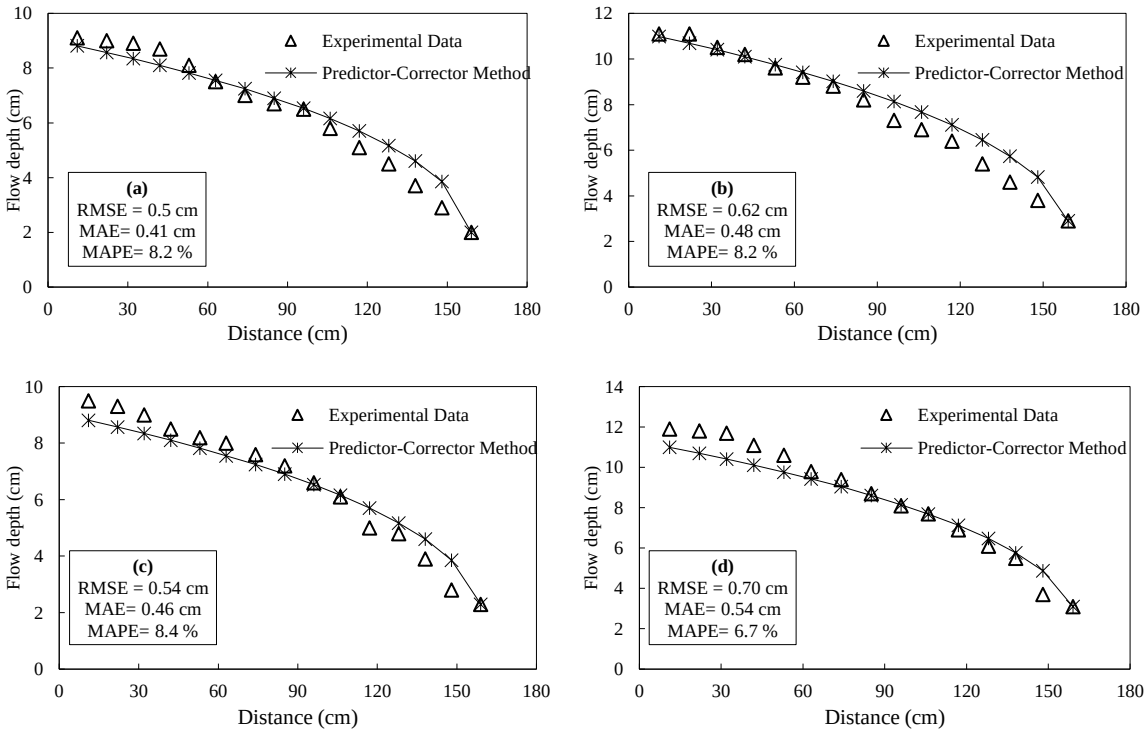

Figure 2. Passing flow profile through the without core rockfill media, a) flow rate 0.26 l/s, d50 = 1.8 cm, b) flow rate 0.37 l/s, d50 = 1.8 cm, c) flow rate 0.26 l/s, d50 = 1.1 cm, d) flow rate 0.37 l/s, d50 = 1.1 cm

The coefficient of determination (R-square), which indicates the correlation between the experimental and numerical data, is equal to 0.98 on average. It can be concluded that the estimation-modification method computes the overall shape of the flow profile very well. From the results of the preliminary tests, it can be concluded that the numerical estimation-modification method is suitable for the flow profile computation. Therefore, it has been used in cases including impermeable cores inside the aggregate medium.

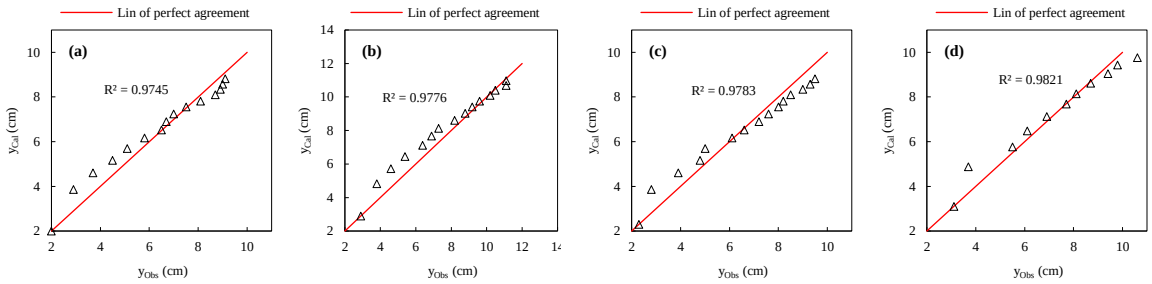

Figure 3. Comparison of observed data and calculation data, a) flow rate 0.26 l/s, d50 = 1.8 cm, b) flow rate 0.37 l/s, d50 = 1.8 cm, c) flow rate 0.26 l/s, d50 = 1.1 cm, d) flow rate 0.37 l/s, d50 = 1.1 cm.

3.2. Flow profile in the presence of an impermeable core

If impermeable cores are inside the rockfill media, the flow profile should be divided into two upstream and downstream parts. In both cases, the gradually varied flow regime is dominant, and only near the core edge, the current overflows from the core, and the curvature of the current is high. Because these two profiles are individual, the boundary conditions should be appropriately considered for each. The boundary condition is adopted in the downstream of each profile. For the downstream profile of the core, the adopted boundary condition is exit flow depth. On the other hand, for the upstream profile, the boundary condition is set to the edge of the core. In the following, the flow profiles in different situations have been calculated.

3.2.1. Flow profile in positions P1, P2 and P3

The cores were installed vertically in positions P1, P2, and P3. S1, S2, and S3 cores were installed separately in each position. In Figs. 4, 5, and 6, flow profiles are shown in positions P1, P2, and P3, respectively.

The calculated errors show an excellent correlation between the experimental data and the calculated profiles by the estimate correction method. Also, the root mean square error (RMSE) for the S1 and S3 cores is calculated as 4.3 and 4.9 mm, respectively, which is acceptable.

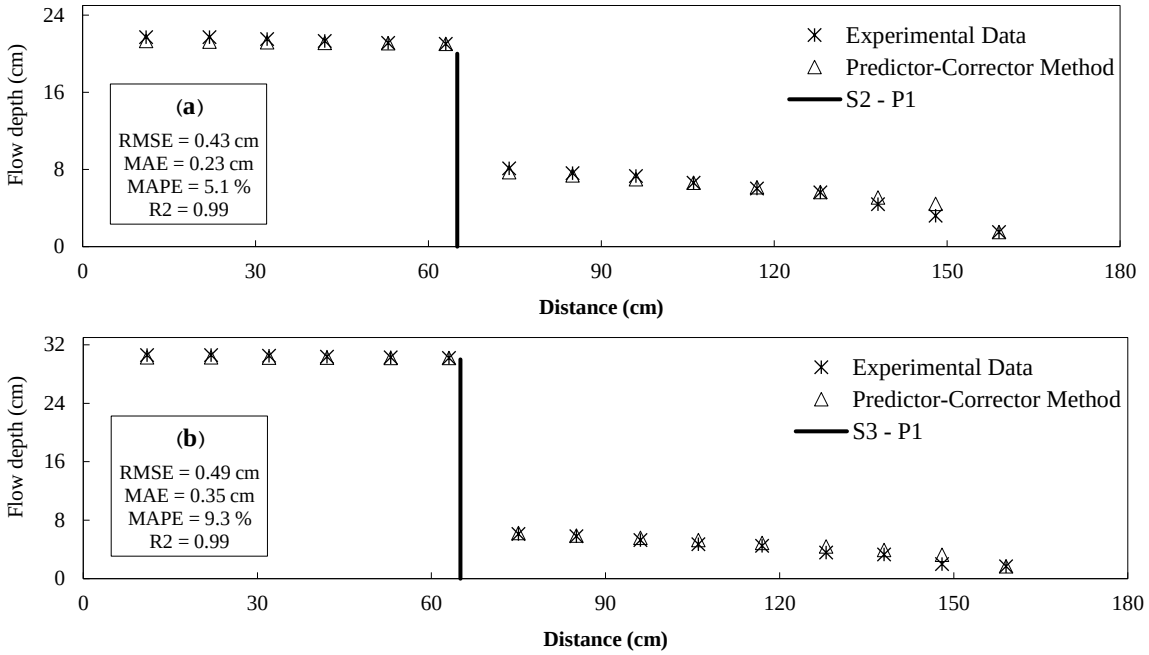

Figure 4. Depiction of water surface profile using experimental data and numerical estimation-correction method in the case of vertical core in position (P1), a) flow discharge 0.26 l/s, b) flow discharge 0.19 l/s

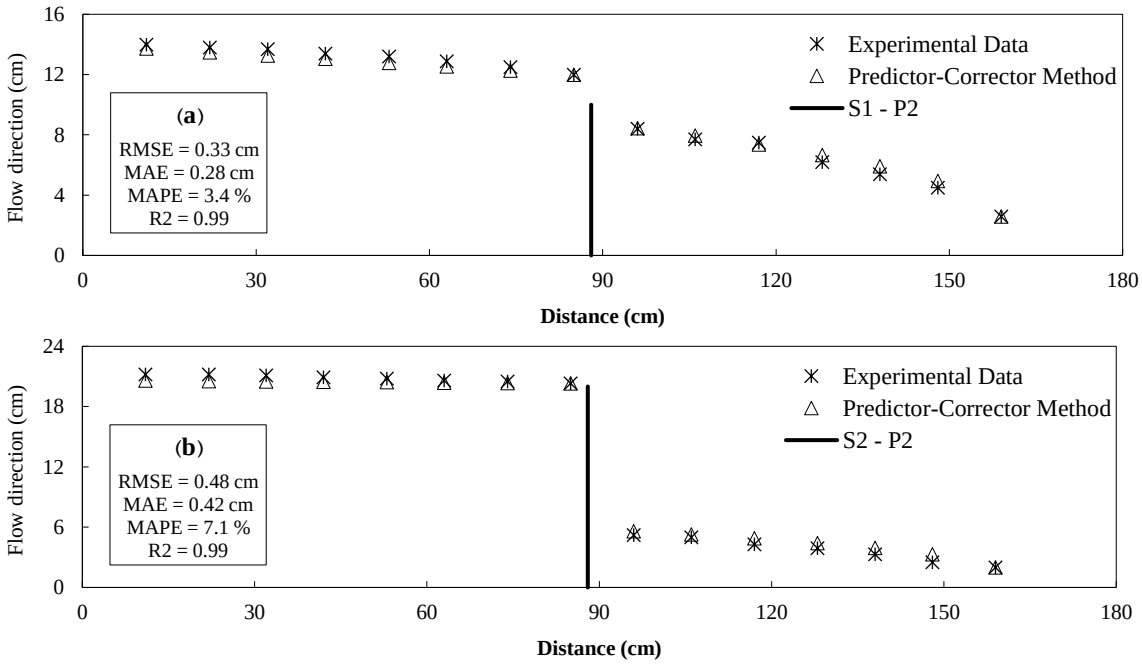

Figure 5. Comparison of depicted water surface profile using laboratory data and estimation-correction numerical method in a vertical core state in position (P2), a) flow rate 0.37 l/s, b) flow rate 0.19 l/s

As is shown in Figs. 4, 5, and 6, the numerical estimation-correction method calculates the surface profile satisfactorily in the presence of vertical cores inside the gravel dam. The root mean square error (RMSE) ranged from 3 to 5.5 mm, and the relative error was calculated between 3 and 9.3 %. Also, the error comparison shows that with the increase in the core height, the error values also increase. This growth is more noticeable downstream of the core. This is because in the vicinity of the core, the flow has local acceleration, and the curvature of the flow is more significant.

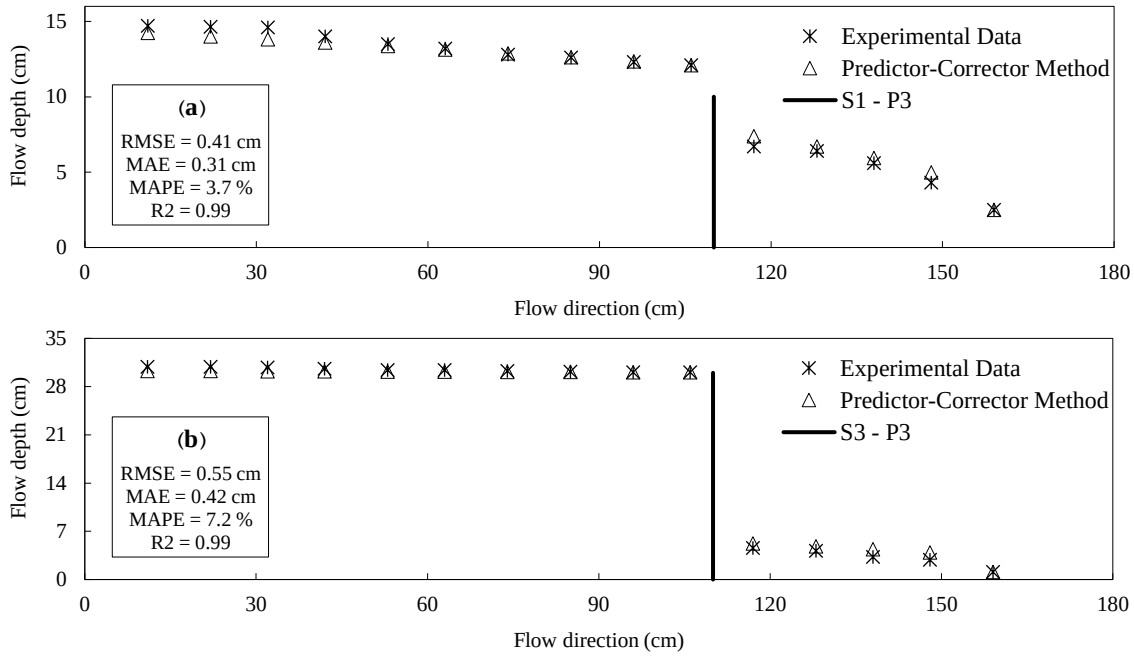

Figure 6. Depiction of water surface profile using laboratory data and estimation-correction numerical method in a vertical core state in position (P2), a) flow rate 0.37 l/s, b) flow rate 0.19 l/s

3.2.2. Flow profile at position P4

In this case, the core encounters the flow and forms an acute angle with the horizon surface. Due to the slope's existence, the current's movement mechanism differs from the vertical core case. If the flow rate is low, the flow slips slowly with contact with the downstream surface of the core. However, the flow falls vertically to the downstream profile for higher flow rates. In Fig. 7, three examples of comparing experimental and numerical results with different flow rates and geometries can be seen in P4.

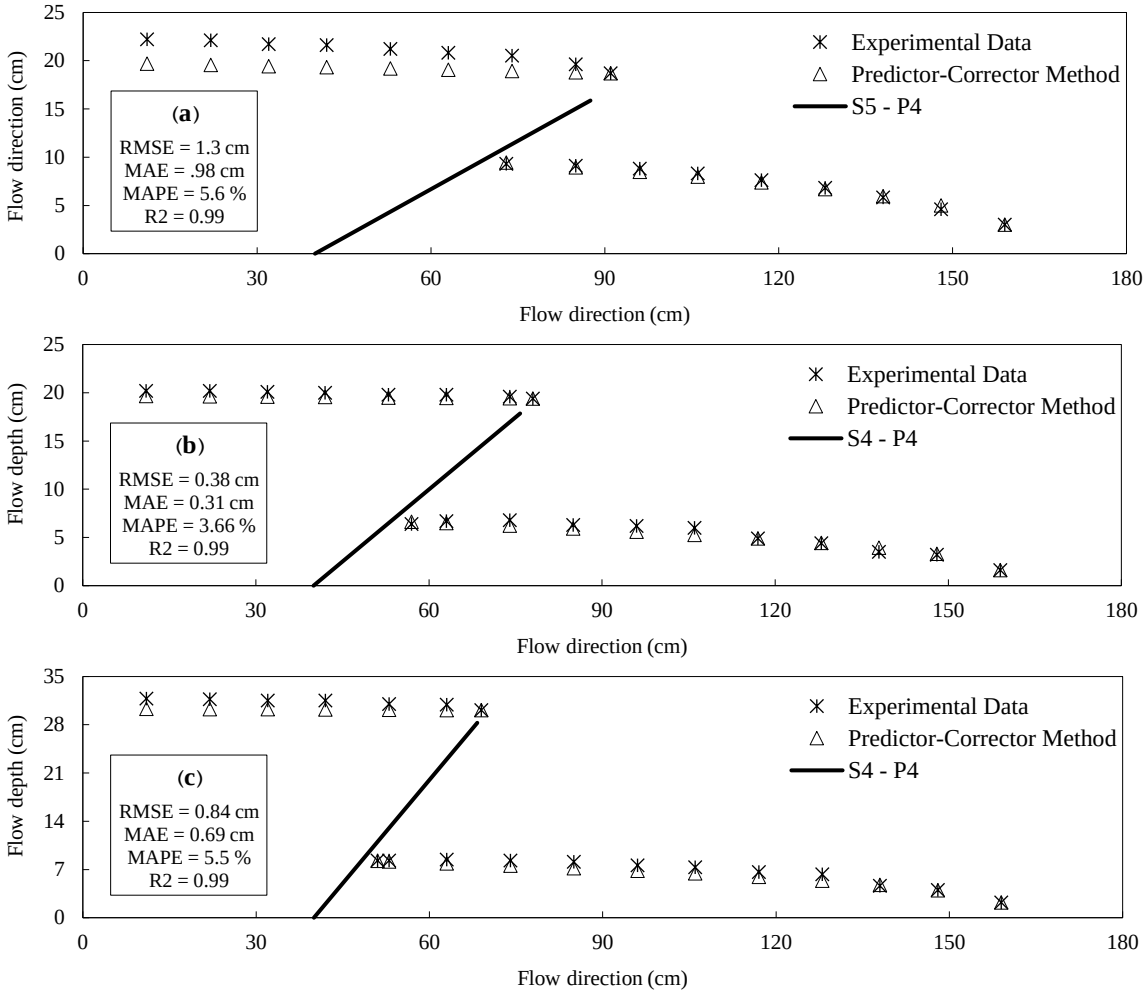

Figure 7. Depiction of flow water surface profile for laboratory data and estimation-correction numerical method in the vertical core state in position (P4).a) flow rate 0.37 l/s, the angle relative to the horizon 18.5 degrees, b) flow rate 0.19 l/s, the angle relative to the horizon 26.5 degrees, c) flow rate 0.26 l/s, the angle to the horizon is 45 degrees.

Error analysis reveals that in the case of an inclined core, the estimation-correction method is less accurate, and the error rate increases with the increase in entrance discharge. It was found that an increase in flow rate increases the flow velocity and local acceleration, especially at the separation point of two profiles, where the curvature of the surface profile is seen. Consequently, the accuracy of the profile computation decreases.

3.2.3. Flow profile at position P5

The inclined core faces the flow at position 5 and forms an acute angle with the horizon in the counterclockwise direction (Fig. 8). In this case, the geometry of the core does not have a considerable effect on the upstream flow, but in downstream it has a significant effect on flow motion pattern inside the rockfill body. This effect is more noticeable at higher flow rates (Fig. 8).

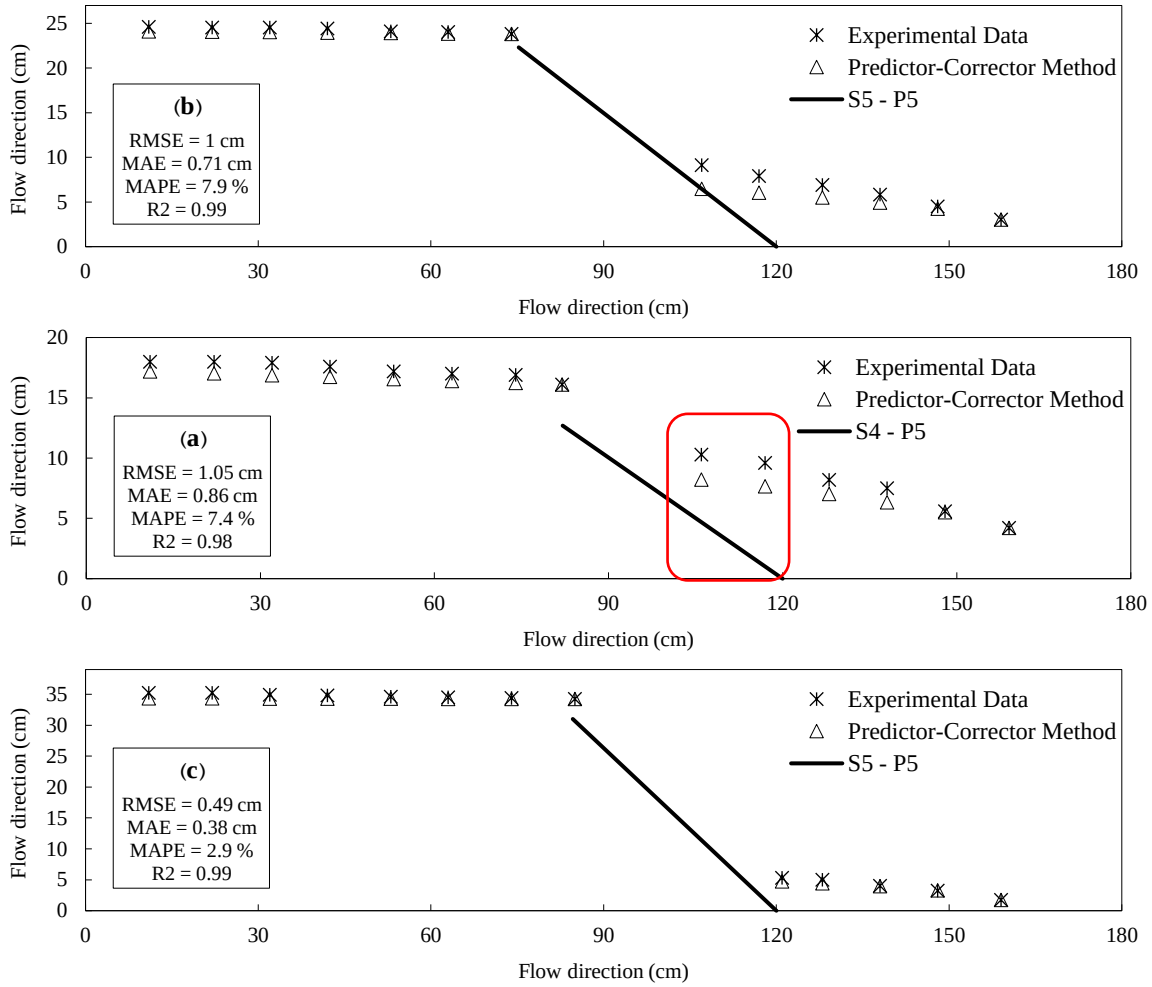

Figure 8. Depiction of water surface profile for laboratory data and numerical estimation-correction method in vertical core mode in position (P5), a) flow rate 0.37 l/s, angle to horizon 18.5 degrees, b) flow rate 0.26 l/s, angle to the horizon 26.5 degrees, c) flow rate 0.19 l/s, angle to the horizon 45 degrees

Fig. 8 shows that at a flow discharge of 0.19 l/s, the relative error is 3%. However, at higher flow rates, this value reaches 8%. Also, the mean square error in the flow rate of 0.37 l/s is 1.1 cm, and for the flow rate of 0.19 l/s, this value is about 0.5 cm. The experimental and the computed profiles using the numerical method of estimation correction are compared by calculating statistical error parameters for all tests (number of tests 63). The detailed results are illustrated in Table 2. Because the number of tests is large and it is not possible to include all of them in the table, the average error parameters for different discharge has been computed. For example, in position 1, the average error of three discharges and three types of core installation (S1, S2, and S3) is averaged and introduced as the error value in position P1.

Table 2. Error values for comparison of laboratory data and numerical solution using estimate-correction method

	Core position				
	P1	**P2**	**P3**	**P4**	**P5**
RMSE (cm)	0.51	0.41	0.48	0.9	0.85
R^2	0.99	0.99	0.99	0.99	0.99
MAPE %	6.4	6.1	6.2	6.6	7.1
MAE (cm)	0.43	0.3	0.32	0.61	0.58

Furthermore, in the extracted analytical relation (Eq. 16), to determine the value of a coefficient to use in the longitudinal profile calculations, it is necessary to use the laboratory results to calibrate it and then evaluate its efficiency. For this purpose, its value is extracted using the least square curve fitting method by taking into account the influencing factors, including the rockfill media diameter, the length of the porous medium, and the operated flow rate for a specific diameter. In the next step, other profiles are calculated and compared with the observed profiles to verify the relationship and obtained value. The comparison results showed that the value of this coefficient does not change by changing the medium's length or the inlet flow rate. Besides, its value for the medium with a rock diameter of 1.8 cm equals 26.5. According to the differences in the flow depth on the porous media, the Reynolds number values ($Re = \frac{uR}{\vartheta}$) would also be variable. As a result, it is necessary to pay attention to the formation or non-Darcy turbulent flow along the entire length of the porous media. The range of calculated Reynolds numbers through longitudinal water surface profiles is 3100 to 11000. It is evident that all are within the range of turbulent flows, and the assumption of the formation of non-Darcy flow is correct. It was also observed that the Reynolds numbers become higher with the increase in discharge and decrease in the porous media length.

4. Conclusion

The application of gradually-varied flow algorithms in simulating buried streams has proven to be an effective and practical approach. By utilizing experimental data and applying the gradually-varied flow theory, water surface profiles have successfully been calculated in various scenarios of non-Darcy flow. In this research, the longitudinal profiles of the water surface were taken in different conditions by conducting a series of experiments in a laboratory flume. Furthermore, a new relationship was presented by analyzing the existing relationships to calculate the flow depth at different longitudinal distances. Coefficients of the presented relationship were calibrated using part of the acquired experimental data. Then, they were used for depth calculation for other laboratory conditions. It was found that in addition to the simplicity of the new relationship, it can be used with acceptable accuracy for predicting the flow profile. Additionally, the flow profile through the porous medium in the presence of inclined and vertical impermeable cores was investigated. The laboratory results were compared with the numerical results, and the error values were calculated. The results showed that the estimated profile by the numerical estimation-correction method has a very high correlation (0.99) with the laboratory data. Also, the average calculated errors indicate the high accuracy of the methods. The computed values for statically RMSE, MAPE, and MAE parameters were calculated as 6.3 mm, 6.5%, and 4.5 mm, respectively. Moreover, it was found that at higher flow rates and in the vicinity of the core edge (the point of profile separation), the flow curvature

was higher, and consequently, the estimation error was higher. In conclusion, the application of gradually-varied flow algorithms in simulating buried streams offers a practical and cost-effective solution for analyzing the behavior of flow in non-Darcy porous media. By combining experimental data, numerical methods, and the gradually-varied flow theory, significant advancements in understanding the complex dynamics of buried streams would be made. This knowledge can be applied to various engineering projects, ensuring the optimal design and operation of hydraulic structures. These findings have significant implications for hydraulic engineering and the design of structures involving buried streams. The ability to accurately predict and simulate the behavior of flow in porous media is crucial for ensuring the safety and efficiency of hydraulic structures.

References

1. Mousavi, S., E. Amiri-Tokaldany, and M. Davoudi, A Relationships to Determine the Critical Hydraulic Gradient and Noncohesive Sediment Transport Discharge in Rockfill Dams. Research journal of Environmental sciences, 2011. 5(5): p. 399.
2. Mohamadiha, A., et al., Numerical and Experimental Study of the Unsteady Flow with Different Distance Steps in Body of Rockfill Dam. Iranian Journal of Irrigation & Drainage, 2018. 11(6): p. 1152-1161.
3. Chabokpour, J. and E. Amiri Tokaldany, Experimental-numerical simulation of longitudinal water surface profile through large porous media. Iranian Water Researches Journal, 2017. 11(3): p. 81-90.
4. Acharya, R.C., S.E. van der Zee, and A. Leijnse, Porosity–permeability properties generated with a new 2-parameter 3D hydraulic pore-network model for consolidated and unconsolidated porous media. Advances in water resources, 2004. 27(7): p. 707-723.
5. Constantinides, G.N. and A.C. Payatakes, Network simulation of steady-state two-phase flow in consolidated porous media. AIChE Journal, 1996. 42(2): p. 369-382.
6. Fischer, U. and M.A. Celia, Prediction of relative and absolute permeabilities for gas and water from soil water retention curves using a pore-scale network model. Water Resources Research, 1999. 35(4): p. 1089-1100.
7. Held, R.J. and M.A. Celia, Pore-scale modeling extension of constitutive relationships in the range of residual saturations. 2001, Wiley Online Library.
8. Herrera, N. and G. Felton, Hydraulics of flow through a rockhll dam using sediment-free water. Transactions of the ASAE, 1991. 34(3): p. 871-0875.
9. Hosseini, S.M. and D. Joy, Development of an unsteady model for flow through coarse heterogeneous porous media applicable to valley fills. International Journal of River Basin Management, 2007. 5(4): p. 253-265.
10. Hansen, D., V.K. Garga, and D.R. Townsend, Selection and application of a one-dimensional non-Darcy flow equation for two-dimensional flow through rockfill embankments. Canadian Geotechnical Journal, 1995. 32(2): p. 223-232.
11. Jeannin, P.Y., Modeling flow in phreatic and epiphreatic karst conduits in the Hölloch cave (Muotatal, Switzerland). Water Resources Research, 2001. 37(2): p. 191-200.
12. Li, B., V.K. Garga, and M.H. Davies, Relationships for non-Darcy flow in rockfill. Journal of hydraulic Engineering, 1998. 124(2): p. 206-212.

13. Stephenson, D., Rockfill in hydraulic engineering. 1979: Elsevier.
14. Chabokpour, J., Application of hybrid cells in series model in the pollution transport through layered material. Pollution, 2019. 5(3): p. 473-486.
15. Thauvin, F. and K. Mohanty, Network modeling of non-Darcy flow through porous media. Transport in Porous Media, 1998. 31(1): p. 19-37.
16. Wang, X., F. Thauvin, and K. Mohanty, Non-Darcy flow through anisotropic porous media. Chemical Engineering Science, 1999. 54(12): p. 1859-1869.
17. Wu, Y.S., An approximate analytical solution for non-Darcy flow toward a well in fractured media. Water Resources Research, 2002. 38(3): p. 5-1-5-7.
18. Chabokpour, J., O. Minaei, and M. Dasineh, Derivation of new analytical solution for pollution transport through large porous media. International Journal of Environmental Science & Technology (IJEST), 2020. 17(12).
19. Bazargan, J., et al., Determination of discharge coefficient of inbuilt spillway in rock-fill dams. 2011.
20. Wilkins, J., Flow of water through rock fill and its application to the design of dams. New Zealand Engineering, 1955. 10(11): p. 382-387.
21. Norouzi, H., et al., Estimating output flow depth from Rockfill Porous media. Water Supply, 2021.
22. Sedghi-Asl, M. and I. Ansari, Adoption of extended Dupuit–Forchheimer assumptions to non-Darcy flow problems. Transport in Porous Media, 2016. 113(3): p. 457-469.
23. Heydari, M. and Z. Khodakaramian, One-Dimensional Discharge-Stage Theory Relationship Modifying in non-Core Rock fill Dams Using Laboratory Model. Advanced Technologies in Water Efficiency, 2022. 1(1): p. 108-120.
24. Salahi, M.-B., M. Sedghi-Asl, and M. Parvizi, Nonlinear flow through a packed-column experiment. Journal of Hydrologic Engineering, 2015. 20(9): p. 04015003.
25. Asiaban, P., E. Amiri Tokaldany, and M. Tahmasebi Nasab, Simulation of water surface profile in vertically stratified rockfill dams. International Journal Of Environmental Research, 2015. 9(4): p. 1193-1200.
26. Sarvarian, J., J.M.V. Samani, and H.M.V. Samani, Two-objective Optimization of Location and Geometric Characteristics of Rockfill Dams at the Taleghan Basin by NSGA-II. Environmental Energy and Economic Research, 2018. 2(4): p. 281-296.
27. Zhang, W., et al., A Critical Review of Non-Darcian Flow and Future Challenges. Earth and Space Science Open Archive ESSOAr, 2020.
28. Reddy, H.P., M.H. Chaudhry, and J. Imran, Computation of gradually varied flow in compound open channel networks. Sadhana, 2014. 39: p. 1523-1545.
29. Chaudhry, M.H., Open-channel flow. Vol. 523. 2008: Springer.